Supplementary Information

Photo-isomerisation of alkenyl complexes of platinum(II): structural, spectroscopic, kinetic, and computational investigations

Carmen R. Barone,[a] Cecilia Coletti,[c] Ruth J. McQuitty,[b] Nicola J. Farrer,[b] Giuseppe Lorusso,[a] Luciana Maresca,[*a] Alessandro Marrone,[c] Giovanni Natile,[a] Concetta Pacifico,[a] Simon Parsons,[d] Nazzareno Re,[c] Peter J. Sadler,[b] and Fraser J. White.[d]

[a] *Dipartimento di Chimica, Università degli Studi "Aldo Moro" di Bari, Via E. Orabona 4, I-70125 Bari, Italy . E-mail: luciana.maresca@uniba.it*

[b] *Department of Chemistry, University of Warwick, Coventry CV4 7AL, U. K.*

[c] *Dipartimento di Farmacia, Università degli Studi "Gabriele d'Annunzio", Via dei Vestini 31, I-06100 Chieti, Italy.*

[d] *School of Chemistry, The University of Edinburgh, King's Building, West Mains Road, Scotland, EH9 3JJ, U. K.*

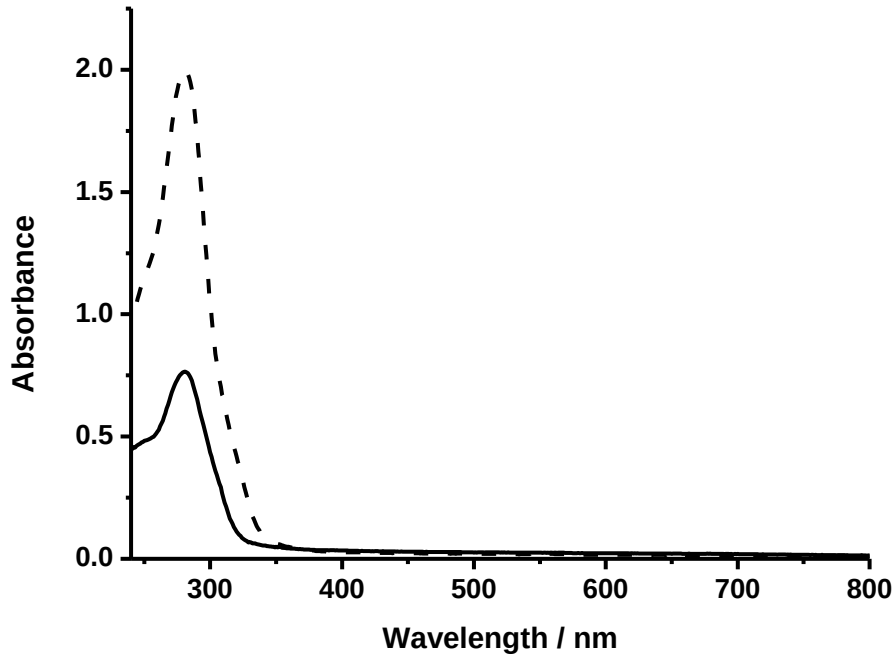

Figure S1. UV-Vis absorption spectrum of 87 µM compound (*E*)-**2a** (solid line) and of 79 µM (*E*)-**2b** (dotted line) in $CDCl_3$.

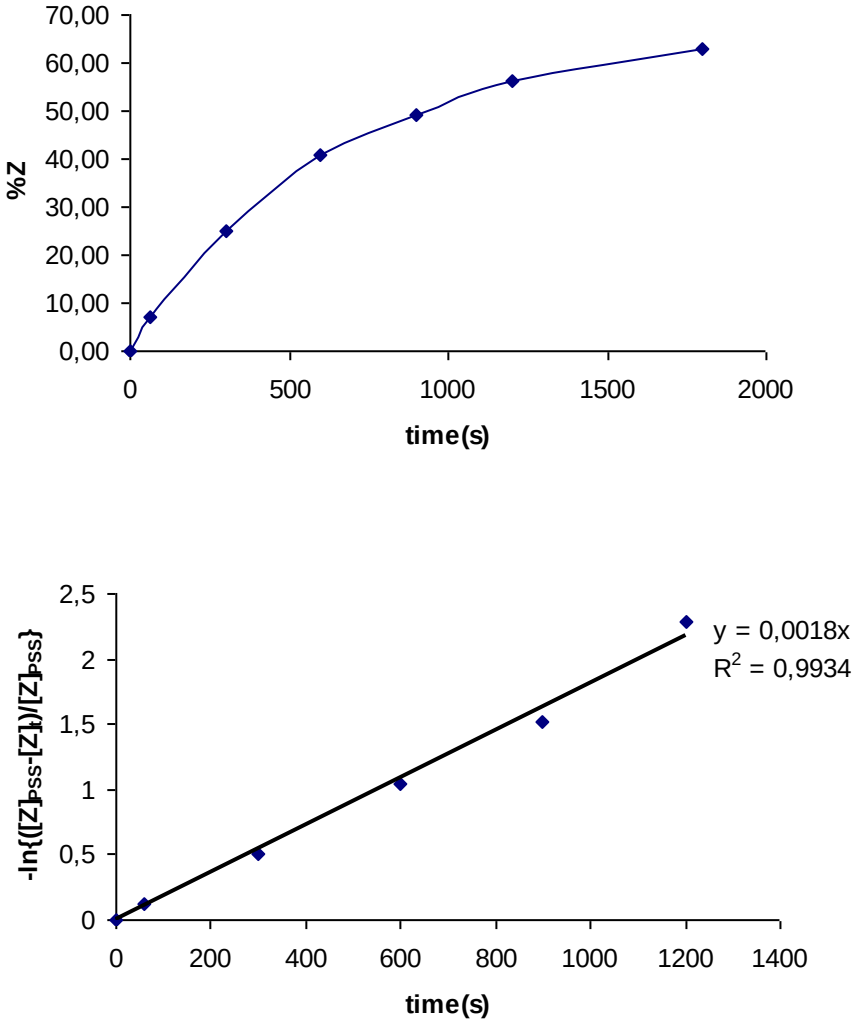

Figure S2. Photo-isomerisation of (*E*)-**2a** (λ = 351 nm). Top: plot of percentage of Z isomer (%*Z*) *versus* time of irradiation (s). Bottom: plot of $-\ln\{([Z]_{PSS}-[Z]_t)/[Z]_{PSS}\}$ against time (s).

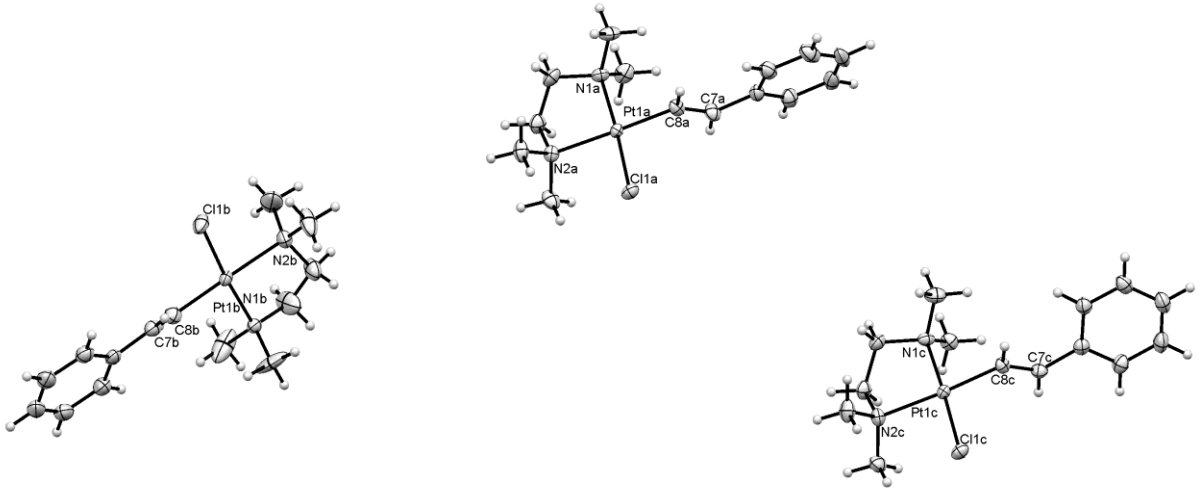

Figure S3. The three independent molecules in the asymmetric unit of compound (*E*)-**2a**. The ellipsoids enclose 50% probability.

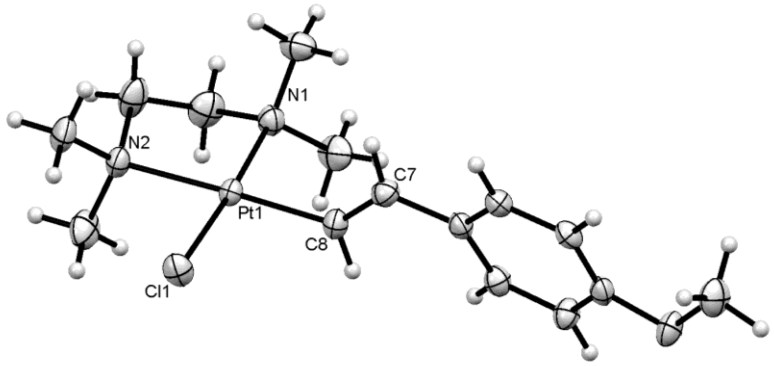

Figure S4. The single molecule in the asymmetric unit of compound (*E*)-**2b**. The ellipsoids enclose 30% probability.

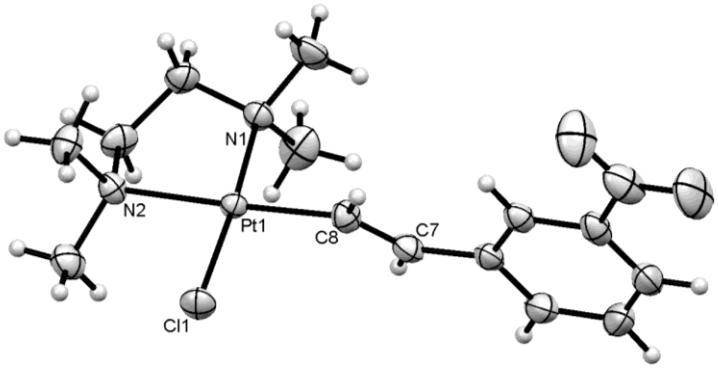

Figure S5. The single molecule in the asymmetric unit of compound (*E*)-**2c.** The ellipsoids enclose 30% probability.

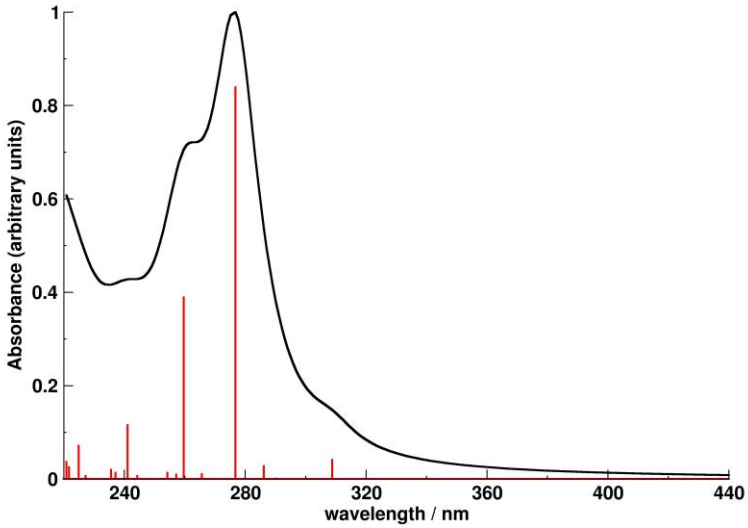

Figure S6. Experimental and calculated UV-Vis spectrum for (*E*)-**2a**.

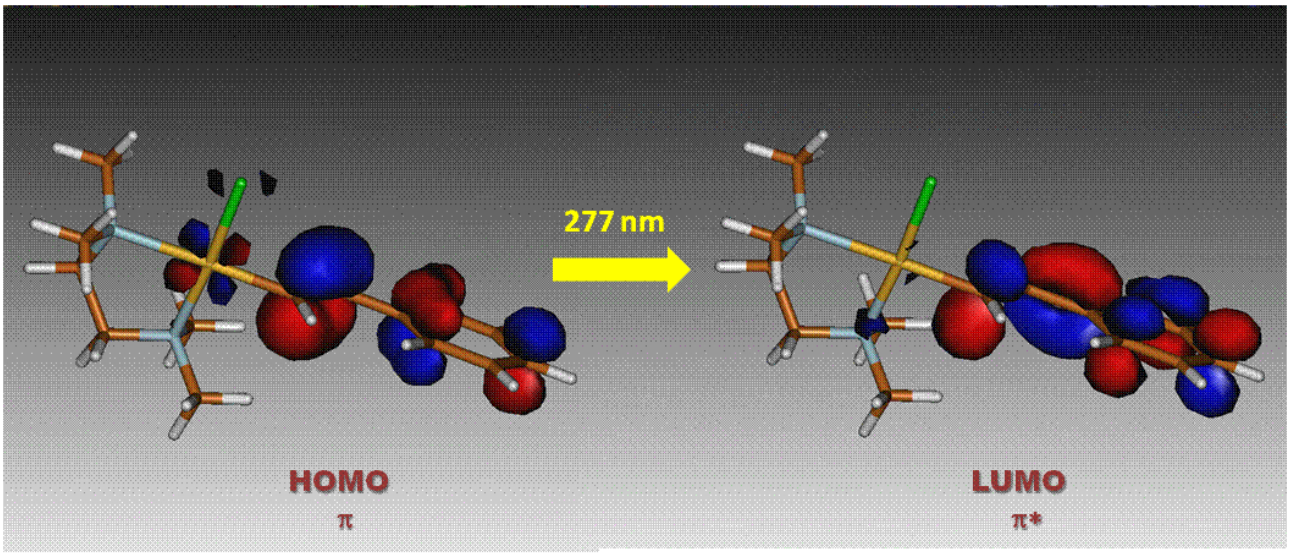

Figure S7. HOMO and LUMO orbitals involved in the π→ π* transition at 277 nm (S_3) for (*E*)-**2a**.

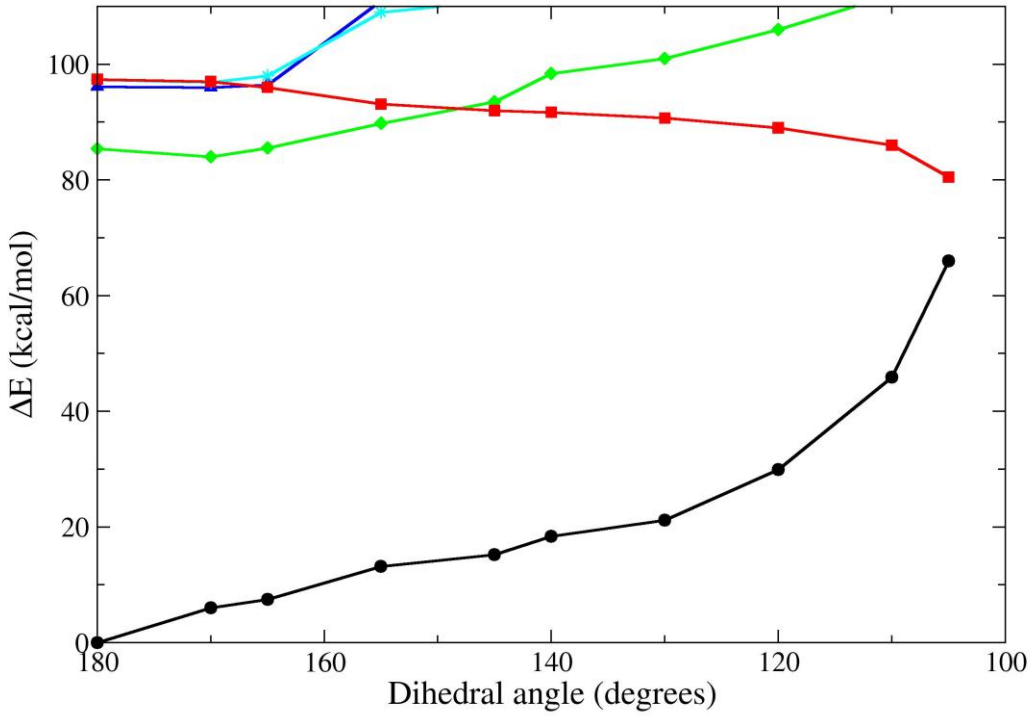

Figure S8. Energy profile for the ground and the four lowest singlet excited state surface of (*E*)-**2a**, as a function of the dihedral angle ϕ around the C=C alkenyl double bond. (S_0 —, S_1 —, S_2 —, S_3 —, S_4 —)

Table S1. Crystallographic data

	(*E*)-**2a**	(*Z*)-**2a**	(*E*)-**2b**	(*E*)-**2c**
Chemical formula	$C_{14}H_{23}ClN_2Pt$	$C_{14}H_{23}ClN_2Pt$	$C_{15}H_{25}ClN_2OPt$	$C_{14}H_{22}ClN_3O_2Pt$
M_r	449.88	449.88	479.91	494.88
Crystal system, space group	Orthorhombic, *Pbca*	Monoclinic, $P2_1/n$	Orthorhombic, $P2_12_12_1$	Monoclinic, *C*2/*c*
a, *b*, *c* (Å)	21.7511 (17), 11.4643 (9), 37.772 (3)	7.9854 (4), 20.2676 (10), 9.6517 (5)	10.0881 (6), 12.1859 (6), 13.5748 (6)	27.2807 (7), 8.1215 (2), 15.6844 (4)
α, β, γ (°)	90, 90, 90	90, 97.931 (3), 90	90, 90, 90	90, 97.426(2), 90
V (Å^3)	9418.8 (13)	1547.14 (14)	1668.79 (15)	3445.89 (15)
Z	24	4	4	8
μ (mm^{-1})	9.10	9.23	8.57	8.31
T(K)	150	150	150	293
Crystal size (mm)	0.90 × 0.30 × 0.14	0.50 × 0.44 × 0.27	0.48 × 0.34 × 0.15	0.17 × 0.12 × 0.03
Absorption correction	Integration + multiscan *XPREP* + *SADABS*	Multi-scan *SADABS*	Multi-scan SADABS	Multi-scan SADABS
T_{min}, T_{max}	0.020, 0.291	0.031, 0.080	0.14, 0.28	0.721, 1.00
No. of measured, independent and observed [$I > 2\sigma(I)$] reflections	135583, 11993, 10157	14968, 4319, 3576	19914, 4104, 3923	32586, 4290, 3364
No. of parameters	487	163	182	194
No. of restraints	0	0	0	0
R_{int}	0.065	0.047	0.034	0.061
$(\sin\theta/\lambda)_{max}$ (Å^{-1})	0.681	0.714	0.680	0.668
$R[F^2 > 2\sigma(F^2)]$, $wR(F^2)$, *S*	0.031, 0.069, 1.08	0.053, 0.131, 1.13	0.018, 0.039, 1.00	0.047, 0.123, 1.02
$\Delta\rho_{max}$, $\Delta\rho_{min}$ (e Å^{-3})	3.18, −1.14	4.70, −3.49	1.35, −0.90	7.76, −0.870
Flack parameter*	–	–	−0.009 (6)	–

* H. D. Flack, *Acta Cryst. A*, 1983, **39**, 876-881.

Table S2. Comparison of the experimental and calculated (with B3LYP, BH-HLYP, PBE and PBE0 functionals) main geometrical parameters for complex (*E*)-**2a.**

	(*E*)-2a (exp.)	B3LYP	BH-HLYP	PBE	PBE0
Pt1-N1	2.068(4)- 2.074(4) -2.072(4)	2.148	2.130	2.128	2.107
Pt1-N2	2.164(4)-2.185(4)- 2.180(4)	2.274	2.241	2.254	2.222
Pt1-Cl1	2.298(1)- 2.305(1)- 2.302(1)	2.313	2.302	2.298	2.284
Pt1-C8	1.984(4)-1.983(5)-1.977(4)	1.992	1.989	1.978	1.974
C8-C7	1.315(7)- 1.322(7) -1.330(6)	1.340	1.328	1.352	1.339
C7-C1	1.479(6)-1.481(7)- 1.475(6)	1.472	1.469	1.470	1.467
N1-Pt1-N2	84.8(2) - 84.4(2) - 84.5(2)	83.28	83.44	83.82	84.03
C8-Pt1-Cl1	90.4(1) - 92.2(1) -91.7(1)	90.16	89.77	90.60	90.17
N2-Pt1-Cl1	92.5(2) - 91.8(1) - 93.0(1)	91.96	92.00	91.52	91.85
C8-Pt1-N1	92.4(2) - 91.9(2) - 90.8(2)	94.59	94.76	94.04	93.96
C7-C8-Pt1	127.4(4) - 131.7(4) - 128.1(4)	127.34	127.43	127.40	127.13
C8-C7-C1	127.5(5) -124.4(5) - 127.1(4)	127.30	127.21	127.31	127.06
A	49.7 - 86.1 - 89.8	78.0	82.2	77.0	78.2
B	25.8 - 5.8 - 23.2	9.5	30.6	4.0	10.2

Table S3. Pt···H_{ortho} distances and Mulliken atomic charges on Pt, Cl and H_{ortho} in $CHCl_3$ solution of (*E*) and (*Z*)-**2a-2d**. For (*Z*)-**2c** and (*Z*)-**2d** the relative energies of the two possible conformers **A** and **B** in Chart 2 are reported. Distances in Ångstrom, energies in kJ mol^{-1}.

Complex	Conf	Distance	Energy	Charges		
		Pt···H_{ortho}		Pt	Cl	H_{ortho}
(*E*)-**2a**		-	-	0.152	–0.326	0.138
(*Z*)-**2a**		2.738	-	0.143	–0.319	0.157
(*E*)-**2b**			-	0.147	–0.329	0.142
(*Z*)-**2b**		2.779	-	0.140	–0.321	0.160
(*E*)-**2c**			-	0.169	–0.320	0.180 / 0.155
(*Z*)-**2c**	**A**	2.461	0.0	0.101	–0.293	0.226 / 0.159
	B	2.715	2.9	0.119	–0.302	0.195 / 0.179
(*E*)-**2d**			-	0.155	–0.326	0.137 / 0.120
(*Z*)-**2d**	**A**	2.633	0.2	0.076	–0.298	0.197 / 0.134
	B	2.764	0.0	0.089	–0.298	0.175 / 0.197

Table S4. Natural bond analysis: summary of second order perturbation theory analysis of Fock matrix in NBO basis. l.p. = lone pair. E(2) = energy contribution (kJ mol^{-1}) to non-Lewis delocalization.

Complex	Conf	Donor NBO	Acceptor NBO	E(2)
(*Z*)-**2a**		π(Pt-Cl)	σ*(C–H_{ortho})	3.1
		d_{z^2} (Pt)	σ*(C–H_{ortho})	4.3
		l.p. (Cl)	σ*(C–H_{ortho})	2.9
(*Z*)-**2b**	**A**	d_{z^2} (Pt)	σ*(C–H_{ortho})	4.1
		l.p. (Cl)	σ*(C–H_{ortho})	3.0
(*Z*)-**2c**	**A**	π(Pt-Cl)	σ*(C–H_{ortho})	3.3
		d_{z^2} (Pt)	σ*(C–H_{ortho})	13.9
(*Z*)-**2c**	**B**	π(Pt-Cl)	σ*(C–H_{ortho})	3.9
		d_{z^2} (Pt)	σ*(C–H_{ortho})	5.9
		l.p. (Cl)	σ*(C–H_{ortho})	3.9
(*Z*)-**2d**	**A**	π(Pt-Cl)	σ*(C–H_{ortho})	3.3
		d_{z^2} (Pt)	σ*(C–H_{ortho})	7.3
(*Z*)-**2d**	**B**	π(Pt-Cl)	σ*(C–H_{ortho})	2.8
		d_{z^2} (Pt)	σ*(C–H_{ortho})	4.3
		l.p. (Cl)	σ*(C–H_{ortho})	2.5

Table S5. Energies and nature of the contributing molecular orbitals for the twenty lowest transitions of (*E*)-**2a**.

Energy	Intensity×100	Electronic transitions		
309 nm	2.04	H → L+1	S_1	($\pi \rightarrow d_{x2-y2}^*$)
290 nm	0,02	H-1 → L+1	S_2	($p_z(Cl) + d_{yz} \rightarrow d_{x2-y2}^*$)
286 nm	1.36	H-2 → L+1	S_3	($d_{z2} \rightarrow d_{x2-y2}^*$)
277 nm	41.2	H → L	S_4	($\pi \rightarrow \pi^*$)
265 nm	0.53	H-4(3) → L+1	S_5	(d_{xz} ($p_x(Cl)+d_{xy}$) $\rightarrow d_{x2-y2}^*$)
260 nm	19.4	H → L+2	S_6	($\pi \rightarrow \pi^*_{phen}$)
257 nm	0.47	H-1 → L	S_7	($p_z(Cl) + d_{yz} \rightarrow \pi^*$)
254 nm	0.65	H-2 → L	S_8	($d_{z2} \rightarrow \pi^*$)
244 nm	0.31	H → L+3	S_9	($\pi \rightarrow \sigma^*_{CH(tmeda)}$)
241 nm	5.71	H-3 → L H-4 → L+1	S_{10}	($p_x(Cl)+d_{xy} \rightarrow \pi^*$) ($d_{xz}$ ($p_x(Cl)+d_{xy}$) $\rightarrow d_{x2-y2}^*$)
237 nm	0.66	H → L+4	S_{11}	($\pi \rightarrow \sigma^*_{CN(tmeda)}$)
236 nm	0.98	H-3 → L H-3 → L +1	S_{12} H-4 → L	($p_x(Cl)+d_{xy} \rightarrow \pi^*$) ($p_x(Cl)+d_{xy} \rightarrow d_{x2-y2}^*$) d_{xz} ($p_x(Cl)+d_{xy}$) $\rightarrow \pi^*$)
227 nm	0.30	H-1 → L+3	S_{13}	($p_z(Cl) + d_{yz} \rightarrow \sigma^*_{CH(tmeda)}$)
225 nm	3.54	H-4 → L	S_{14}	d_{xz} ($p_x(Cl)+d_{xy}$) $\rightarrow \pi^*$)
222 nm	1.23	H-1 → L+4	S_{15}	($p_z(Cl) + d_{yz} \rightarrow \sigma^*_{CN(tmeda)}$)
221 nm	1.81	H-2 → L+3 H-1 → L+4	S_{16}	($d_{z2} \rightarrow \sigma^*_{CH(tmeda)}$) ($p_z(Cl) + d_{yz} \rightarrow \sigma^*_{CN(tmeda)}$)
217 nm	8.30	H-5 → L	S_{17}	($\pi_{arom} \rightarrow \pi^*$)
216 nm	0.11	H-1→ L+2	S_{18}	($p_z(Cl) + d_{yz} \rightarrow \pi^*_{phen}$)
214 nm	2.23	H-2 → L+4	S_{19}	($d_{z2} \rightarrow \sigma^*_{CH(tmeda)}$)
212 nm	2.21	H-2 → L+2	S_{20}	($d_{z2} \rightarrow \pi^*_{phen}$)